ADVANCED MATERIALS TECHNOLOGIES
www.advmattechnol.de

Printed Humidity Sensors from Renewable and Biodegradable Materials

Xavier Aeby, James Bourely, Alexandre Poulin, Gilberto Siqueira, Gustav Nyström, and Danick Briand**

Increasing environmental concerns raised by the accumulation of electronic waste draws attention to the development of sustainable materials for short-lived electronics. In this framework, printed capacitive humidity sensors and temperature resistive detectors composed exclusively of biodegradable materials: shellac, carbon-derived particles, and egg-albumin are reported. The sensor platform comprises interdigitated electrodes serving as a capacitive transducer for humidity sensing, and a serpentine used as a resistive temperature detector. Both the interdigitated and serpentine electrodes are manufactured by screen-printing carbon ink on a shellac substrate. The humidity sensors are constructed by drop-coating egg albumin on the interdigitated carbon electrodes and the temperature detector is prepared by encapsulating the serpentine design with shellac. Shellac is shown to be a biodegradable alternative to hydrophilic cellulose-derived substrates, with the capacitive humidity sensors demonstrating a sensitivity of 0.011% RH^{-1}. The response and recovery times on shellac are 12 and 20 times faster than on cellulose-based substrate, and the serpentine resistive temperature detectors have a temperature coefficient of 5300 ppm K^{-1}. At the end of their service-life, the sensors produced are home compostable and can be environmentally friendly disposed, potentially enabling their future use for sustainable and environmentally friendly smart-packaging, agricultural sensing, or point-of-care testing.

1. Introduction

With recent advances in the area of the Internet-of-Things (IoT), a new class of short service-life and single-use electronic devices is emerging.[1] Devices with such features require a paradigm shift from traditional electronics notably regarding materials and manufacturing to minimize electronic waste.[2,3] One key application for such biodegradable electronics is smart packaging.[4] This field is thriving from the exponentially growing internet commerce (e-commerce) activities and can provide interactive features such as position tracking or environmental parameters monitoring.[5] The latter has a crucial influence on perishable or pharmaceutical goods, and monitoring humidity and temperature fluctuation would help to prevent and reduce losses. Significant efforts have been undertaken to develop environmental sensing platforms to monitor the supply chain and decrease food or drug waste.[6] Commercially available examples include re-usable platforms[7] or complex radio frequency identification (RFID)-based systems[8] and are yet to be single-use or biodegradable.

Relative humidity sensors rely on capacitive or resistive measurements.[9] Capacitive sensors are well adapted for single-use, low-power, and disposable electronics due to their design simplicity and wide measurement range. They consist of a substrate and a humidity sorption layer (i.e., sensing layer) usually coated on top of planar transducing electrodes such as interdigitated electrodes (IDEs).[10] The total capacitance of IDEs is given by the electrostatic contribution of each neighboring electrode and varies with modification of the dielectric properties of the sensing layer or substrate, due to water molecules sorption. Printed capacitive humidity sensors are demonstrated on various plastic foils, including polyethylene terephthalate (PET),[11] polyimide (PI),[12] parylene (PN),[13] and polypropylene (PP).[14] While their processing can be compatible with large area manufacturing for large volume production, they are not biodegradable. Cellulose substrates, such as paper and cardboard, are also used as substrates for humidity sensors.[15] Cellulose is the most abundant organic polymer on the planet and is biodegradable.[16] However, the roughness of cellulose-based substrates is often detrimental to the electrical conductivity of printed electrodes,[17] and the

X. Aeby, A. Poulin, G. Siqueira, G. Nyström
EMPA
Swiss Federal Laboratories for Materials Science and Technology
Cellulose & Wood Materials Laboratory
Dübendorf 8600, Switzerland
E-mail: gustav.nystroem@hest.ethz.ch

J. Bourely, D. Briand
École Polytechnique Fédérale de Lausanne (EPFL)
Soft Transducers Laboratory (LMTS)
Neuchâtel 2000, Switzerland
E-mail: danick.briand@epfl.ch

G. Nyström
Department of Health Sciences and Technology
ETH Zürich
Schmelzbergstrasse 9, Zürich 8092, Switzerland

The ORCID identification number(s) for the author(s) of this article can be found under https://doi.org/10.1002/admt.202201302.

DOI: 10.1002/admt.202201302

inherent hygroscopicity of cellulose fibers can affect the sensor performance.[17]

High sensitivity and fast response/recovery time are the two important requirements for the sensing layer. High-performance sensing materials for a capacitive sensor include functionalized poly (methyl methacrylate) (PMMA)[18] and structures based on metal oxides.[19] Several researchers have also been successful in implementing biodegradable materials such as carboxymethyl cellulose,[20] cellulose nano-fibrils,[21] proteins,[22] silk,[23] or starch[24] as substrates. However, processing sensors made of fully biodegradable materials remains a challenge to address. In fact, most of the reported works implement silver, copper, or gold as IDEs. Silver has been shown to contribute to 80% of the total toxicity of silver-based RFID devices[25] and requires passivation for stable operation.[26] Thus, the use of silver materials should be minimized in single-use electronics, while gold is expensive to implement in low-cost devices and copper is challenging to print due to oxidation of copper particles.

Here, we report on a fully printed and disposable environmental sensing platform made of carbon transducers applied to humidity and temperature sensing. Interdigitated carbon electrodes coated with a humidity-sensitive layer for capacitive humidity sensing and a carbon resistor for temperature sensing are processed by printing on a shellac substrate. Shellac is a natural, renewable and biodegradable resin, well known as a hydrophobic coating for wood surfaces. While shellac already finds commercial application as an edible protective coating against humidity in the food industry, its use for disposable electronics remains limited to the application as a dielectric layer for organic transistors[27] and as carbon-loaded current collectors for supercapacitors.[28] In this paper, we demonstrate that shellac is less sensitive to humidity compared to cellulose-based substrates. This in turn leads to an enhanced sensitivity and response time of IDEs on shellac coated with egg albumin (EA) as a humidity sensing layer compared to the same device architecture on cellulose-derived substrate. Our sensing platform, composed exclusively of biodegradable materials for temperature and humidity sensing, sheds light on how to assemble environmental-friendly materials for the creation of high-performance sustainable sensors.

2. Results and Discussion

2.1. Material Properties and Sensor Manufacturing

The process flow to manufacture the sensors is illustrated in **Figure 1**a. Both sensors are fabricated by solution casting the shellac substrate; screen-printing both carbon electrodes (i.e., the IDEs for the humidity sensors and the serpentine for the temperature detector); drop-casting the egg albumin active layer on top of the IDEs for the humidity sensor; and spray-coating the shellac encapsulation layer on top of the serpentines for the temperature detector. The resulting humidity and

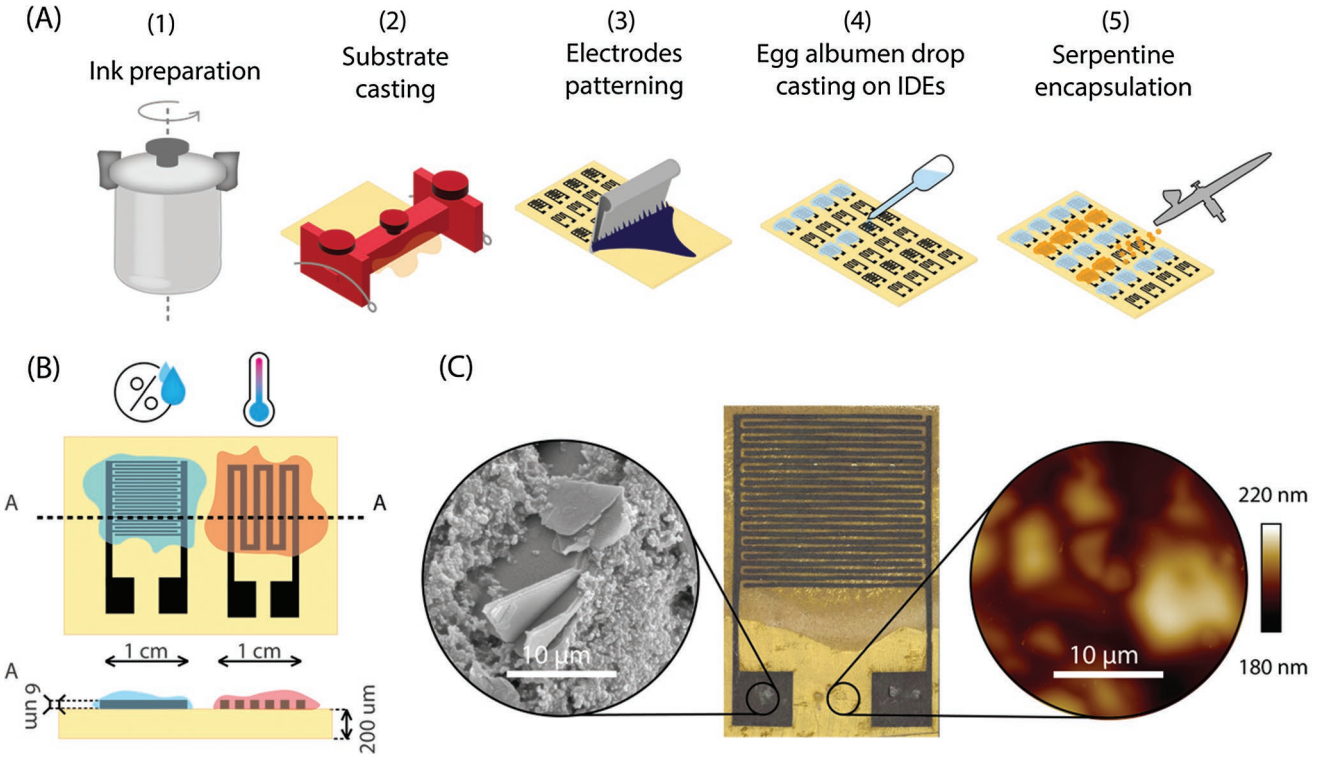

Figure 1. A) Schematic of the fabrication process, showing the 5 main steps, consisting of: 1) ink preparation for the substrate and the electrically conductive ink; 2) preparation of the shellac substrate using a film applicator; 3) patterning of the temperature and humidity sensors using screen-printing; 4) drop-casting egg albumin as a humidity sorption layer for the IDEs; 5) encapsulation of the resistive sensors by spraying a shellac solution. B) Schematic of the sensor platform concept, showing the principal dimensions. C) Picture of the IDEs on shellac substrate showing a high-resolution picture of the disposable sensor and a finger resolution of 200 µm underneath the coating of 5 wt% egg-albumin solution. The left inset shows the two carbon particles' morphology of the ink and the right inset shows the atomic-force-microscopy height sensor image.

temperature sensors have an active footprint of 1 cm^2 each. The design of the sensors is schematized in Figure 1b and the complete design is visible in Figure S1a (Supporting Information). The humidity sensor, with the egg-albumin coating, is shown in Figure 1c, with an inset of the electrodes providing a scanning electron microscopy image of the electrode and an inset of the substrate morphology.

The ≈200 µm thick shellac substrate is cast from a solution of ethanol:pentanol (1:1). Pentanol provides a lower vapor pressure than a pure ethanol solution, thus enabling a lower casting speed of ≈1 cm s^{-1} which improves film uniformity. Shellac forms a smooth substrate with an arithmetic surface roughness of 50 nm measured on a 100 μm^2 sample area, as shown in Figure S1b (Supporting Information). The arithmetic roughness measured by contact profilometry and Atomic-Force-Microscopy (AFM) is comparable to printed electronics substrates.[17,29] To assess the effect of shellac as a substrate on the performance of the sensor, carbon electrodes were also printed onto glass and paper substrates. Glass was considered as an inorganic and non-biodegradable reference due to its low water absorption properties, while paper is the main biodegradable substrate used in printed electronics.

The carbon ink contains graphite flakes and carbon-black dispersed in a shellac matrix as shown previously.[28] The graphite flakes provide high electrical conductivity media, connected by the carbon black particles. Carbon materials are intrinsically hydrophobic, chemically stable and undergo negligible oxidation. Due to their lack of water absorption and limited oxidation, carbon materials are ideal to produce humidity sensor IDEs. **Figure 2**a,b shows oscillatory and constant shear rheology curves of the electrode ink. The ink exhibits a shear-thinning behavior and a yield shear stress of 75 Pa, typically required for screen-printing. The shear-thinning behavior might emanate from the shellac matrix and the alignment of graphite flakes with shear forces. It lowers the apparent force needed to push the material through the mesh and yields a higher printing resolution. After drying, the resulting printed layer thickness is 6.09 ± 2.95 µm, 5.56 ± 0.96 µm, and 5.73 ± 1.4 µm on glass, paper, and shellac respectively (n = 3). The profile is shown in Figure S1c (Supporting Information). The electrical conductivities, without shellac encapsulation of the carbon features on shellac, glass and paper are 1027 ± 89, 1029 ± 108, and 975 ± 89 S m^{-1} (n = 13), respectively, as shown in Figure 2c. The electrical conductivities are in the same range with a similar standard deviation. Nevertheless, the 5% lower conductivity on the paper substrate is probably caused by the inherent higher porosity and surface roughness of the cellulosic substrate.

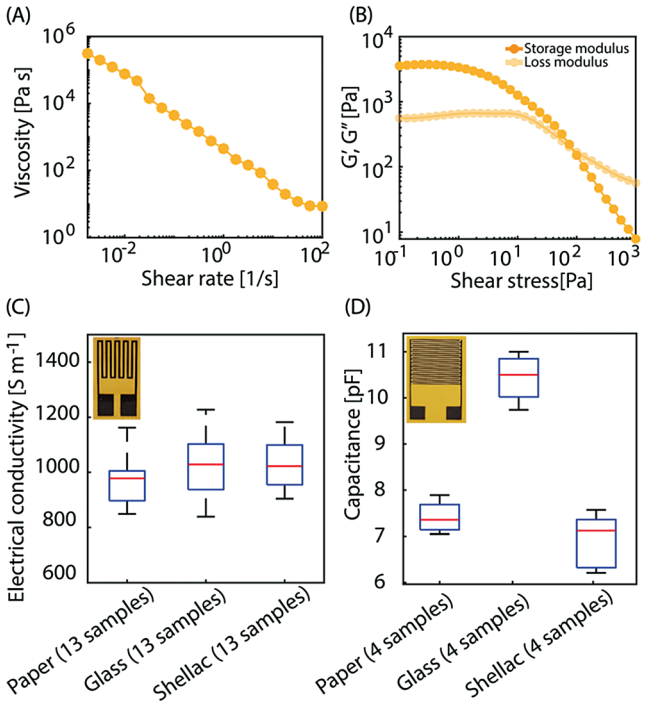

Figure 2. A,B) Oscillatory and constant shear rheology of the carbon, graphite, and shellac ink. The ink exhibits a shear-thinning behavior and a yield shear stress of 75 Pa. C) Electrical conductivity of the printed carbon, graphite, and shellac ink as a function of the type of substrate, inset shows the serpentine design on shellac substrate. Average values of 13 samples. D) Capacitance of the printed IDEs coated with 5% egg albumin as a function of the type of substrate, inset shows the IDEs design on shellac substrate. Average values of 4 samples.

The gap size between fingers and the width of the fingers were set to be equal to 200 µm to reach a fabrication yield of nearly 100%. After the device fabrication, the distance between the IDEs fingers on paper, shellac and glass are 186 ± 12 µm, 194 ± 7 µm, and 168 ± 16 µm and the lines' width are 214 ± 12 µm, 206 ± 7 µm, and 234 ± 16 µm respectively (n = 10). The variation in gap size can be explained by the interaction between the carbon ink and the substrate. For instance, in the case of a glass substrate, the surface energy is higher leading to a more pronounced bleeding effect of the ink and thus a reduction in the gap size.

The permittivity of the glass slide, shellac, and paper substrate was measured to be ε_{paper} = 4.9, $\varepsilon_{shellac}$ = 4.2, and ε_{glass} = 9.3. By following the computational model by Igreja and Dias[30] and using the measured permittivity of glass, shellac, and paper, we can estimate the capacitor value of the IDE structure for a given finger and gap size. Implementing the experimental dimensions for the IDEs with a carbon thickness of 6 µm on a sensing area of 1 cm^2 and a substrate thickness of 200 µm, using the measured permittivity values, we calculate capacitances of 5.7, 5.1, and 9.3 pF for paper, shellac, and glass structures respectively. Without egg-albumin coating, pristine capacitance values for the transducers after manufacturing are 6.6 ± 0.3 pF, 5. ± 0.4 pF, and 9.5 ± 0.1 pF (n = 4) for the paper, shellac, and glass, respectively, and are shown in Figure S2a (Supporting Information). As the geometrical parameters, such as the electrode width and gap of the sensors are similar, the difference in initial capacitance is explained by the various dielectric properties of the underlying substrate. Comparing to the simulated capacitance, the highest variation for measured capacitance comes from the paper-based interdigitated structure with a 16% difference to the model, while smaller differences of 2% and 3% are found for shellac and glass, respectively. A possible explanation is that part of the carbon ink is absorbed inside the paper substrate and the empirical model would need to be adjusted to account for this.

The humidity-sensitive layer exclusively contains egg albumin and is casted from a 5 wt% water solution. As the shellac is insoluble in water, it prevents the penetration of water from the egg-albumin solution into the substrate. The measured thickness of egg albumin on all substrates is ≈5 µm. As expected, the measured capacitances after egg-albumin

coating on paper, shellac and glass are higher at 7.4 ± 0.4 pF, 6.9 ± 0.6 pF, and 10.4 ± 0.5 pF, respectively, as shown in Figure 2d.

2.2. Sensor Characteristics

The dynamic response of uncoated humidity transducers (i.e., the substrate without egg-albumin coating) was evaluated in a gas-mixing chamber and the results are presented in Figure S3a (Supporting Information). The shellac and glass substrates alone show weak response to humidity. Both transducers exhibit a 3% change of the relative capacitance from 35 to 65% RH. This effect can be either due to adsorption of water molecules at the substrate surface, which would affect the dielectric properties in close vicinity of the IDEs; or to small dimensional changes of the carbon electrodes. The paper substrate however, absorbing humidity in itself, exhibits a 28% variation of its relative capacitance from 35 to 65% RH.

The dynamic response of the humidity sensors with egg-albumin coating on glass, paper and shellac was also evaluated using a gas-mixing system. The results for different relative humidity levels are shown in **Figure 3**a. The response for the different substrates as a function of the capacitance is given in the curve of Figure 3c–e. All the coated sensors with egg-albumin exhibit a non-linear response, which is derived from water vapor sorption and diffusion behavior. The total relative capacitance change from 35 to 65% RH is of 24% on glass, 34% on shellac and 50% on paper. If we consider two regimes, from 35 to 50% RH and from 35 to 65% RH, the sensitivities are 0.003 and 0.008% RH^{-1} for glass, 0.003 and 0.011% RH^{-1} for shellac and 0.010 and 0.017% RH^{-1} for paper. The sensor on paper has a higher sensitivity because paper, being sensitive to humidity, contributes to the response.

The sensor dynamic characteristics are presented in Figure 3b with the response and recovery times for different types of substrate used. The response times from 35% to 65% relative humidity are 41.1 ± 2.9 s, 100.5 ± 4.9 s, and 1297.6 ± 37.2 s on glass, shellac, and paper respectively for a flow of 500 mL min^{-1} and a chamber volume of 30 mL. Despite being less sensitive, the sensor on shellac substrate has the main advantage of having a response time 13 times faster than the paper sensor. The sensors recover faster than they respond with recovery times from 65% to 35% relative humidity of 13.1 ± 0.4 s, 12.0 ± 1.9 s, and 789.4 ± 8.6 s on glass, shellac, and paper, respectively. The slower response and recovery on paper is due to the paper substrate itself being sensitive to humidity. The paper substrate being much thicker than the egg-albumin coating, leads to slower water absorption/desorption and diffusion processes. The average reversibility at 35% RH was measured to be 0.3% for shellac, 0.6% for paper, and 0.7% for glass (n = 6, measured with 3 cycles from 50 to 35% RH and 3 cycles from 65 to 35% RH).

The static response of the humidity sensors with egg-albumin coating on paper and shellac was also evaluated in a climatic chamber at 30, 50, and 70% RH, at temperatures of 15, 25, and 35 °C. Their responses across the full cycle are visible in Figure S4b (Supporting Information). **Figure 4**a shows

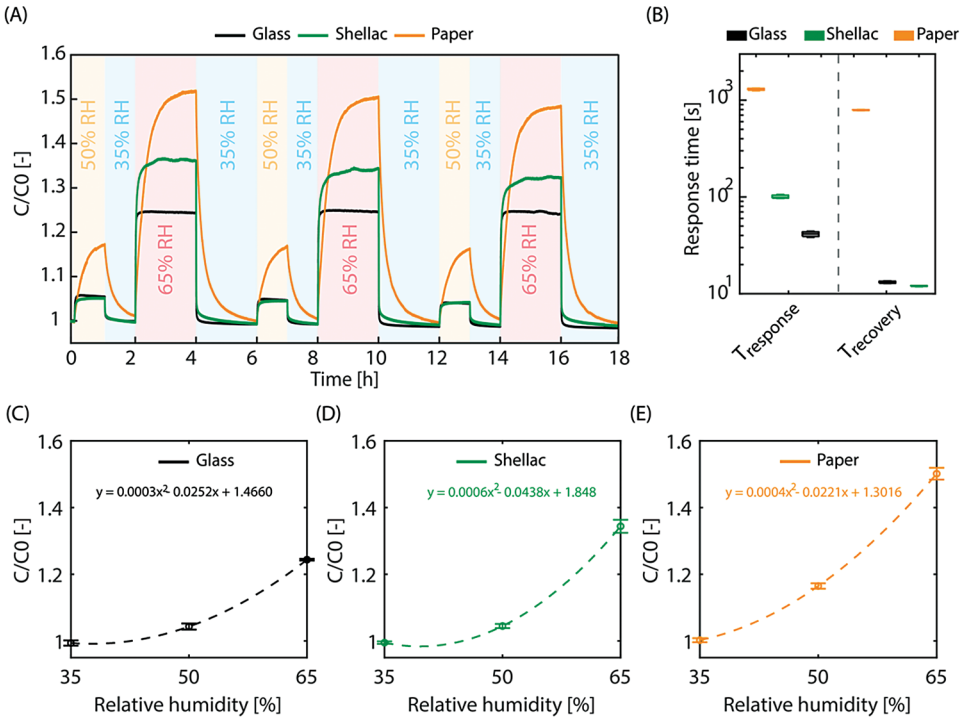

Figure 3. A) Relative capacitance as a function of the time when varying relative humidity for coated IDEs with egg-albumin on glass, paper and shellac, respectively. B) Response and recovery time for the glass, shellac and paper respectively. C–E) Relative capacitance as a function of the relative humidity for the glass, shellac, and paper substrates, showing a non-linear relationship. The dashed lines are second-order polynomial fit for 35 to 65% RH.

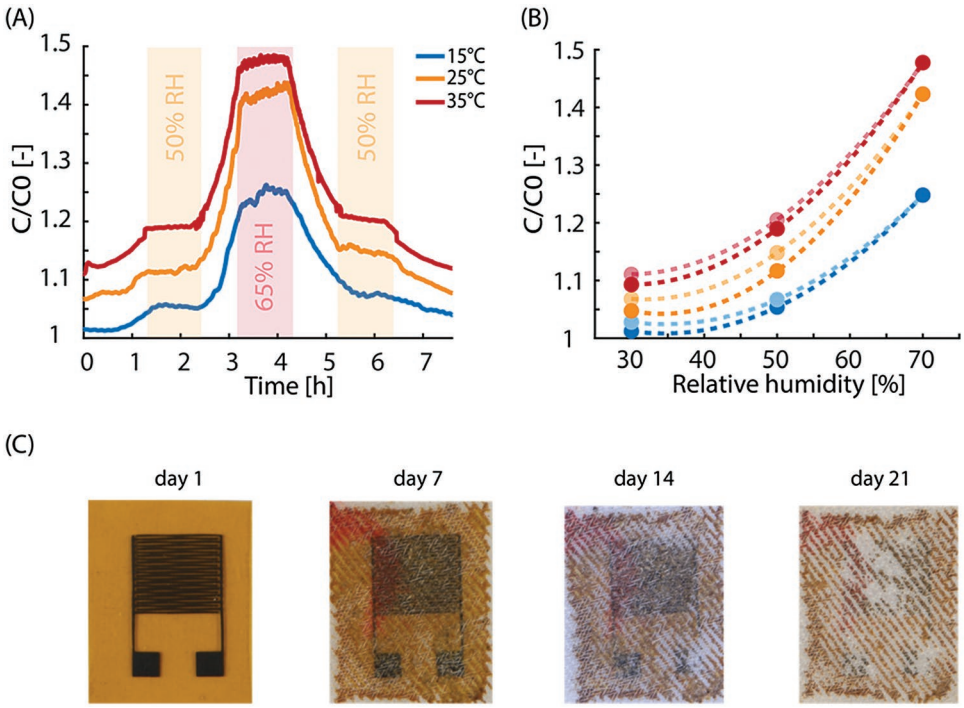

Figure 4. A) Relative capacitance for the sensor on shellac substrate as a function of the time going from 30 to 70% RH at 15, 25, and 35 °C. B) Relative capacitance as a function of the relative humidity, showing the hysteresis for shellac-based humidity sensors at 30, 50, and 65% RH. C) Disintegration of the capacitive sensor on shellac in aerobic composting condition.

the measured capacitance at 15, 25, and 35 °C for humidity ranging from 30 to 70% RH for the egg albumin coated on shellac. As expected, over the full humidity range, the capacitor value changed by an increasing factor of 1.2, 1.4, and 1.5, at 15, 25 and 35 °C, respectively. This behavior is due to the amount of water in air (i.e., the absolute humidity in g m^{-3}) increasing with temperature for a given relative humidity percentage, as can be seen in Figure S4a (Supporting Information). In tests conducted at 25 °C, the change in capacitance with a ratio of 1.4 at 70% RH is coherent with the ratio (1.36) observed in the dynamic test performed at 65% RH.

Figure 4b depicts the capacitance variation and hysteresis at various temperature conditions for the egg-albumin-coated shellac device. The values were calculated by averaging the recorded capacitance during each step of the humidity plateau. The hysteresis of the sensor on shellac substrate from 30 to 70% RH (i.e., the maximum capacitance delta between up and down cycle) is of 1.2%, 2.2%, and 0.9% for 15, 25, and 35 °C respectively. In the case of the paper-based sensor, the hysteresis of the sensor from 30% RH to 70% is of 2.9%, 5.1% and 4.1% for 15, 25, and 35 °C, respectively. The higher hysteresis for paper can be correlated to the diffusion of the humidity within the bulk of the substrate as discussed previously for the dynamic tests performed in the gas mixing setup.

To demonstrate the sustainable character of our materials and humidity sensors, we carried out disintegration tests, which indicate that the sensors can be discarded in a compost condition. The sensors (n = 4) disintegrate as shown in Figure 4c and lose 84.5% of its mass within 77 days as visible in Figure S5 (Supporting Information). Carbon is mostly unaffected by composting but it is a non-toxic element. It can be either collected and reused for other inks preparation and recycled, or simply processed with the organic matter produced by the compost.

To be able to compensate for the temperature dependence of our humidity sensors, we propose to apply the same carbon ink to fabricate a resistive temperature detector with a serpentine shape. Considering a carbon thickness of 6 µm and for a serpentine design 100 mm long and 500 µm wide, we targeted a resistance value of about 35 kΩ. After manufacturing, with a line width slightly lower at 478 ± 17 µm, the resistance achieved after printing and curing is of 38.47 ± 3.25 kΩ. The shellac encapsulation increases the resistance up to 100 kΩ, caused by the interaction of the encapsulation with the conductive composite. **Figure 5**a shows the response of the serpentine to temperature variation from 20 to 35 °C at 50% RH and the relative resistance as a function of the temperature at 35, 50, and 65% RH is shown in Figure 5b–d. The average temperature coefficient (TCR) of the sensors for these three humidity levels is 5309 ppm K^{-1} with a standard deviation of ±159 ppm K^{-1}.

3. Conclusion

We presented an environmentally friendly humidity and temperature sensor exclusively composed of biodegradable materials. We implemented shellac as a novel biodegradable and inert substrate for capacitive humidity sensing with an overall limited contribution to the sensor response in comparison to cellulosic substrates. When coating with an egg-albumin

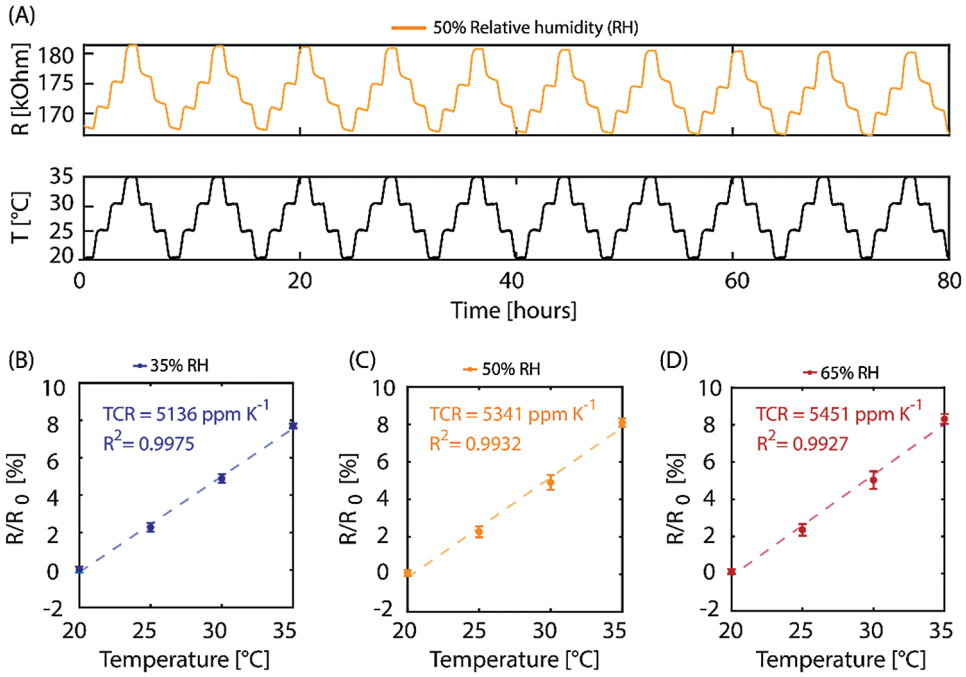

Figure 5. A) Temperature response of the temperature sensor on shellac substrate at 50% RH, showing an increase of electrical resistance with an increase of temperature. B–D) Relative variations showing a similar TCR of 5136 ppm K^{-1} at 35% RH, 5341 ppm K^{-1} at 50% RH and 5451 ppm K^{-1} at 65% RH.

humidity-sensitive coating, the sensor dynamic response and recovery was significantly faster (≈20 times) than on paper substrate with a sensitivity of 0.011% RH^{-1}. The temperature sensor made from a green carbon ink formulation exhibits a temperature coefficient of resistance of 5300 ppm K^{-1}, and besides measuring temperature, could be eventually applied to compensate for the temperature dependence on the humidity sensor response. The ability to use renewable and nontoxic materials for environmental sensing is particularly interesting for smart packaging or warehouse monitoring, and is a step toward sustainable, durable and disposable electronics.

4. Experimental Section

Substrate Preparation: Shellac (dewaxed shellac from Kremer Pigmente, Germany) was dissolved in ethanol and pentanol at a ratio of 2:1:1 for 2 h at 90 °C. Polyethylene glycol (PEG 400 from VWR, Switzerland) at 1.5 wt% of the solid content was added to plasticize the dried shellac films. The solution was manually cast with a 10 cm blade applicator (Zehnter, Switzerland) with blade spacing of 500 µm on a Teflon film. The casting lasts 20 s for a 20 cm film. The paper used was a paper for electronics (XD paper, ArjoWiggins France).

Electrode Ink Preparation: 4.5 g of shellac (dewaxed shellac from Kremer Pigmente, Germany), 1.4 g of carbon black (Carbon ECP from Lion Specialty chemicals, Japan), 3.6 g of graphite (7–10 µm flakes from Alfa Aesar, USA), 7.5 g of pentanol, and 7.5 g of ethanol were mixed for 2 min at 2350 rpm in a speed mixer (DAC600 by Hauschild SpeedMixer, Germany) to ensure uniform dispersion of the carbon particles. The combined materials were processed further for a total of 10 min at 800 rpm in a planetary ball mill (Pulverisette 7 by Fritsch, Germany).

Rheology: The rheometer (MCR 302 rheometer from Anton Paar, USA) was used with a plate–plate geometry with a 1 mm gap and 15 mm plate diameter. All the measurements were carried out at 20 °C. In addition, a solvent-trap was used to prevent evaporation. Viscosity curves were obtained with a sweep of the shear rate from 0.01 to 100 s^{-1} sampled four times per decade. The oscillatory measurements were carried out at 1 Hz, from 0.1% to 1000% deformation sampled at eight points per decade.

Electrode Patterning: Glass, paper, and shellac were cleaned using isopropanol. The carbon–shellac ink was deposited through a 120–30Y polyester mesh (Sefar PME, Switzerland) using a manual screen printer (Novacentrix, USA) with a distance to the substrate of 1 mm. The printed layer was then cured at 60 °C overnight in an oven for all three substrates.

Conductivity Measurements: 13 samples were measured in a two-wire configuration (DMM6500 multimeter, Keithley, USA) with the following formula. As the resistance was high enough, it was considered that the contact resistance would not influence the measurements.

$$\sigma = \frac{1}{R}\frac{L}{S} \tag{1}$$

where σ is the electrical conductivity, R the resistance, L the length of the conductive track, and S the section of the conductive track.

Active Layer Drop-Casting: A micropipette (Eppendorf, Germany) was used to deposit 15 µm of 5 wt% EA solution onto the 1 cm^2 active area of the interdigitated electrodes. The coated device was left to dry at 4 °C in the fridge for over 12 h to prevent cracking of the egg-albumin layer.

Geometrical Measurements: The width of the printed carbon tracks and IDE gap size were measured using a confocal microscope (Keyence, Japan), 3 samples per substrate were measured with 10 measurements per sample. The gaps and fingers width were then averaged per substrate material. The thicknesses of the printed carbon–shellac tracks and the egg albumin were measured using a confocal microscope (Keyence, Japan). The roughness of shellac was obtained with an Atomic-force-microscopy (Bucker, USA) in tapping mode.

Capacitance and Permittivity Model: Theoretical capacitance was computed using the empirical model for an interdigitated capacitor.[21]

$$C_{\mathrm{IDE}_{\mathrm{theory}}} = (N-3)\frac{C_{\mathrm{I}}}{2} + 2\frac{C_{\mathrm{I}}C_{\mathrm{E}}}{C_{\mathrm{I}}+C_{\mathrm{E}}} \tag{2}$$

$$C_I = \varepsilon_o L\left(\frac{K(k_{linf})}{K(k'_{linf})} + \varepsilon_{substrate}\frac{K(k_{linf})}{K(k'_{linf})}\right) \text{where } k_{linf} = \sin\left(\frac{\pi}{2\eta}\right) \text{and } \eta = \frac{W}{W+G} \approx 0.5 \quad (3)$$

$$C_E = \varepsilon_o L\left(\frac{K(k_{Einf})}{K(k'_{Einf})} + \varepsilon_{substrate}\frac{K(k_{Einf})}{K(k'_{Einf})}\right) \text{where } k_{Einf} = \frac{2\sqrt{\eta}}{1+\eta} \quad (4)$$

$$k'_i = \sqrt{1-k_i^2} \quad (5)$$

where $\varepsilon_{substrate}$ is the relative permittivity of the substrate, L = 10.1 mm is the length of the finger, W and G are the finger and gap widths, and N = 24 is the total amount of fingers. K is the complete elliptic integral of first kind[30] with modulus k.

Permittivity Measurement: The permittivity of substrate materials was obtained by measuring the plate capacitor values of glass, paper and shellac dielectric sheets of known thickness by probing with a precision impedance analyzer (Agilent 4294A) at a frequency of 100 kHz. Testing was done at room temperature and 40% RH. The clamping was done mechanically using spring-loaded connectors (Agilent 16034E) made of copper with a flat surface area of 1 mm^2. Permittivity values were extracted from the measured capacitance with respect to the dielectric sheet layer thickness d and averaged across n = 4 measurements for each material:

$$\varepsilon_{dielectric} = \frac{C_{measured} * d}{A * \varepsilon_o} \quad (6)$$

Capacitance Measurement: The capacitive reading was obtained by probing with a LCR meter (Agilent E4980A precision, USA). Capacitance measurements were recorded every second at 100 kHz frequency and 1 V. The cables were calibrated for short and open circuits before probing the interdigitated capacitive electrodes.

Dynamic Response Test: A custom-made gas mixing system composed of a compressed air bottle, gas flow meters (F-201CV-500 from Bronkhorst), a bubbler and a small chamber was used to characterize the devices under various humidity conditions. The flow used to cycle the different atmospheric concentrations was 500 mL min^{-1} for a chamber volume of 30 mL. A primary flow was used to rapidly cleanse the chamber for dynamic characterization of the humidity sensor and characterization was conducted for 27 h.

Static Test: Static testing in a climatic chamber at various temperatures ranging from 15 to 35 °C and relative humidity values between 30 and 70% RH were realized over 54 h. The measurement of the thermal coefficient of resistivity was performed in a controlled environment using a climatic chamber. A humidity and temperature sensor (SHT3x series by Sensirion AG Switzerland) with a resolution of ±2% RH and 0.2 °C was used as a reference to monitor the different chambers used in this study. The response time and recovery time were measured at 67% of the saturation.

Disintegration Test: The international standard from the International Organization of Standardization 20 200 was followed to evaluate the disintegration rate of the sensors under simulated aerobic composting conditions in a laboratory-scale test. It was carried out in the soil, at 58 °C for 77 days. The soil was composed of sawdust, rabbit feed, cornstarch, sugar, corn oil, urea, and compost. The sample was put inside a protective mesh and buried completely in the soil. The mass of the sample was then weighed with and without the protective mesh in week 1, 2, 3, 4, 5, 6, and 9.

Supporting Information

Supporting Information is available from the Wiley Online Library or from the author.

Acknowledgements

The authors kindly acknowledge Nico Kummer and Anja Huch for the help with the AFM and SEM respectively. The authors kindly acknowledge funding from the Swiss National Science Foundation and Innosuisse BRIDGE Discovery program for the project "GREENsPACK—Green Smart Packaging" (Grant No.: 40B2-0_187223/1).

Conflict of Interest

The authors declare no conflict of interest.

Author Contributions

X.A. and J.B. contributed equally to this work. X.A. and J.B. designed and conducted all the experiments. X.A. prepared the substrate, the ink and manufactured the sensor. J.A. prepared the egg-albumin coating and characterized the sensors. All authors analyzed the results, contributed to and reviewed the manuscript writing. All authors have given approval to the final version of the manuscript.

Data Availability Statement

The data that support the findings of this study are available from the corresponding author upon reasonable request.

Keywords

egg albumin, green electronics, humidity sensor, screen-printing, shellac

Received: August 8, 2022
Revised: September 28, 2022
Published online: November 14, 2022

[1] P. Matta, B. Pant, *J. Eng. Sci. Technol.* **2019**, *14*, 1717.
[2] E. R. Rene, M. Sethurajan, V. Kumar Ponnusamy, G. Kumar, T. N. Bao Dung, K. Brindhadevi, A. Pugazhendhi, *J. Hazard. Mater.* **2021**, *416*, 125664.
[3] A. K. Awasthi, J. Li, L. Koh, O. A. Ogunseitan, *Nat. Electron.* **2019**, *2*, 86.
[4] R. Accorsi, M. Bortolini, G. Baruffaldi, F. Pilati, E. Ferrari, *Procedia Manuf.* **2017**, *11*, 889.
[5] S. Chen, S. Brahma, J. Mackay, C. Cao, B. Aliakbarian, *J. Food Sci.* **2020**, *85*, 517.
[6] H. Yousefi, H. M. Su, S. M. Imani, K. Alkhaldi, C. D. Filipe, T. F. Didar, *ACS Sens.* **2019**, *4*, 808.
[7] S. Pfoser, M. Brandner, K. Herman, E. Steinbach, P. Brandtner, O. Schauer, *LOGI – Sci. J. Transp. Logist.* **2021**, *12*, 159.
[8] K. Zannas, H. El Matbouly, Y. Duroc, S. Tedjini, *IEEE Trans. Microwave Theory Tech.* **2018**, *66*, 5885.
[9] H. Farahani, R. Wagiran, M. N. Hamidon, *Sensors* **2014**, *14*, 7881.
[10] Z. Chen, C. Lu, *Sens. Lett.* **2005**, *3*, 274.
[11] F. Molina-Lopez, D. Briand, N. F. De Rooij, *Sens. Actuators, B* **2012**, *166–167*, 212.
[12] G. Mattana, T. Kinkeldei, D. Leuenberger, C. Ataman, J. J. Ruan, F. Molina-Lopez, A. V. Quintero, G. Nisato, G. Tröster, D. Briand, N. F. De Rooij, *IEEE Sens. J.* **2013**, *13*, 3901.
[13] C. Y. Lee, G. W. Wu, W. J. Hsieh, *Sens. Actuators, A* **2008**, *147*, 173.
[14] R. Park, H. Kim, S. Lone, S. Jeon, Y. W. Kwon, B. Shin, S. W. Hong, *Sensors* **2018**, *18*, 1857.
[15] M. Mraović, T. Muck, M. Pivar, J. Trontelj, A. Pleteršek, *Sensors* **2014**, *14*, 13628.

[16] G. Siqueira, J. Bras, A. Dufresne, *Polymers* **2010**, *2*, 728.
[17] D. Tobjörk, R. Österbacka, *Adv. Mater.* **2011**, *23*, 1935.
[18] Y. Sakai, Y. Sadaoka, M. Matsuguchi, *Sens. Actuators, B* **1996**, *35*, 85.
[19] J. R. McGhee, J. S. Sagu, D. J. Southee, P. S. A. Evans, K. G. Upul Wijayantha, *ACS Appl. Electron. Mater.* **2020**, *2*, 3593.
[20] C. Pinming, N. Sukgorn, T. Suhatcho, B. Saetang, P. Kerdkhong, T. Maboonchuay, K. Chalapat, K. Siraleartmukul, *2016 13th Int. Conf. Electr. Eng. Comput. Telecommun. Inf. Technol, ECTI-CON 2016*, **2016**, p. 4.
[21] A. Rivadeneyra, A. Marín-Sánchez, B. Wicklein, J. F. Salmerón, E. Castillo, M. Bobinger, A. Salinas-Castillo, *Compos. Sci. Technol.* **2021**, *208*, 108738.
[22] M. U. Khan, G. Hassan, J. Bae, *Sci. Rep.* **2019**, *9*, 5824.
[23] Y. Luo, Y. Pei, X. Feng, H. Zhang, B. Lu, L. Wang, *Mater. Lett.* **2020**, *260*, 126945.
[24] E. Wawrzynek, C. Baumbauer, A. C. Arias, *Sensors* **2021**, *21*, 6557.
[25] E. Glogic, R. Futsch, V. Thenot, A. Iglesias, B. Joyard-Pitiot, G. Depres, A. Rougier, G. Sonnemann, *ACS Sustainable Chem. Eng.* **2021**, *9*, 11691.
[26] U. Altenberend, F. Molina-Lopez, A. Oprea, D. Briand, N. Bârsan, N. F. De Rooij, U. Weimar, *Sens. Actuators, B* **2013**, *187*, 280.
[27] M. Irimia-Vladu, E. D. Głowacki, G. Schwabegger, L. Leonat, H. Z. Akpinar, H. Sitter, S. Bauer, N. S. Sariciftci, *Green Chem.* **2013**, *15*, 1473.
[28] A. Poulin, X. Aeby, G. Siqueira, G. Nyström, *Sci. Rep.* **2021**, *11*, 11919.
[29] J. Noh, D. Yeom, C. Lim, H. Cha, J. Han, J. Kim, Y. Park, V. Subramanian, G. Cho, *IEEE Trans. Electron. Packag. Manuf.* **2010**, *33*, 275.
[30] R. Igreja, C. J. Dias, *Sens. Actuators, A* **2004**, *112*, 291.